Effects of VIP on Corneal Reconstitution and Homeostasis following *Pseudomonas aeruginosa* Induced Keratitis

Elizabeth A. Berger, Kerry S. Vistisen, Ronald P. Barrett, and Linda D. Hazlett

Purpose. Studies from our laboratory have demonstrated that vasoactive intestinal peptide (VIP) directly converts the normally susceptible C57BL/6J (B6) mouse to resistant after ocular infection through modulation of the inflammatory response. This study examines mechanisms by which VIP influences the healing phase following infection—specifically reconstitution of the extracellular matrix (ECM).

Methods. B6 mice received daily intraperitoneal (IP) injections of VIP, while control mice were similarly injected with sterile phosphate buffered saline (PBS). Real-time RT-PCR, ELISA, and immunofluorescent staining were used to assess the effects of VIP treatment on ECM molecule expression after *Pseudomonas aeruginosa*-induced keratitis. We also compared the effect of VIP treatment on lipopolysaccharide (LPS)-stimulated B6– and BALB/c-derived fibroblasts.

Results. In vivo analyses revealed that VIP treatment of *P. aeruginosa*-infected B6 corneas led to a significant increase in ECM molecules associated with healing/homeostasis, while those associated with ECM degradation were significantly down-regulated when compared to wild-type (WT) controls. In vitro studies revealed that VIP treatment of lipopolysaccharide-stimulated fibroblasts derived from susceptible B6 and resistant BALB/c mice expressed distinct differences in ECM molecule expression, whereby the latter expressed higher levels of ECM molecules aimed at reconstitution. Furthermore, differential expression of VIP receptor-1/VIP receptor-2 (VIPR1/VIPR2) was observed between B6 and BALB/c after VIP treatment of LPS-stimulated fibroblasts.

Conclusions. VIP treatment functions to enhance ECM reconstitution, which appears to be carried out in large part by fibroblasts via VIPR2. Overall, the data from this study suggest that VIP not only regulates disease pathogenesis, but also functions to restore integrity of the corneal stroma. (*Invest Ophthalmol Vis Sci.* 2012;53:7432–7439) DOI:10.1167/iovs.12-9894

Pseudomonas aeruginosa (*P. aeruginosa*) is a common, opportunistic, gram-negative pathogen well-associated with induction of microbial keratitis, especially in patients who are immunocompromised (secondary to malnutrition, alcoholism, diabetes, steroid use), those who have undergone refractive corneal surgery, and in extended wear contact lens (CL) wearers.[1,2] Of the more than 30 million CL wearers in the United States alone, these patients comprise up to 42% of bacterial keratitis cases. Despite the advent of new lens materials, there has been no reduction in disease incidence.[3] While overnight or extended wear remains the major risk factor, recent evidence has revealed that water sources, lens care products, and hygiene are particularly relevant to the pathogenesis of these infections, as well.[4]

As the most significant complication of CL wear, microbial keratitis is an inflammatory ulceration of the cornea (epithelium or stroma) secondary to microbial infection and host response. Clinical presentation includes corneal infiltrate with or without significant tissue loss; dense, suppurative stromal inflammation and edema; increased anterior chamber reaction with or without hypopyon; and mucopurulent exudate. Successful disease resolution depends not only on bacterial clearance, but on the regulation of immune cells, balance between pro- and anti-inflammatory factors released by these cells and the microenvironment, and effective restoration of tissue homeostasis. Previous studies from our laboratory have provided evidence that vasoactive intestinal peptide (VIP), an endogenous neuropeptide produced by several types of neurons and immune cells, influences disease pathogenesis as it relates to bacterial keratitis. We have demonstrated a role for VIP in the modulation of inflammatory cells and mediators including macrophages (MΦ), cytokines, chemokines,[5] Toll-like receptors (TLRs), and TLR-related molecules (Szliter EA, et al. *IOVS* 2008;49:ARVO E-Abstract 2477). Recently, we have provided compelling evidence that VIP influences the corneal microenvironment by regulating adhesion molecules throughout the corneal epithelium, stroma, and endothelium.[7] In summary, this selective modification was shown to mitigate the transmigration of inflammatory cells, which ultimately precluded corneal perforation.

The consequences of bacterial keratitis include the destruction of the extracellular matrix (ECM) by proteolytic enzymes associated with both the bacteria and host response.[8] While it has been evinced that VIP is a potent regulator of the proinflammatory aspect of disease pathogenesis, how this neuropeptide affects the restoration of the ECM or promotes corneal healing has yet to be determined. As such, the study described herein utilizes a well-established murine model of bacterial keratitis to begin elucidating the in vivo effects of VIP treatment regarding healing and reconstitution of the ECM; the second part of the study is an in vitro analysis of how fibroblasts in particular respond to the effects of VIP.

Materials and Methods

Experimental Animal Protocol

Eight-week-old female B6 mice (C57BL/6J; The Jackson Laboratory, Bar Harbor, ME) were housed according to National Institutes of Health

From the Department of Anatomy and Cell Biology, Wayne State University School of Medicine, Detroit, Michigan.

Supported by National Institutes of Health Grants R01 EY002986 (LDH), P30EY004068 (LDH), and MEBTC (EAB).

Submitted for publication March 21, 2012; revised July 12, July 31, August 28, and September 11, 2012; accepted September 22, 2012.

Disclosure: **E.A. Berger**, None; **K.S. Vistisen**, None; **R.P. Barrett**, None; **L.D. Hazlett**, None

Corresponding author: Elizabeth A. Berger, Department of Anatomy and Cell Biology, Wayne State University School of Medicine, 540 E. Canfield Avenue, Detroit, MI 48201; eberger@med.wayne.edu.

guidelines. Mice were anesthetized using ethyl ether, and the left cornea was wounded as previously described.[9] Infection was experimentally induced by delivering a 5-μL aliquot containing 1×10^6 CFU of *P. aeruginosa* (Strain 19660; American Type Culture Collection, Manassas, VA) to the ocular surface of the wounded eye. Subsequently, eyes were examined at 24 hours after infection (PI) and/or times described below to ensure that mice were similarly infected and to monitor disease progression. All animals were treated in accordance with the ARVO Statement for the Use of Animals in Ophthalmic and Vision Research, and all research was approved by the Wayne State University Animal Institutional Review Board.

VIP Treatment

Regarding in vivo studies, B6 mice received daily intraperitoneal (IP) injections of VIP, 5 nM in 100 μL, (VIP; Bachem Americas, Inc., Torrance, CA) beginning 1 day prior to infection through 5 days PI. Control mice were similarly injected with sterile PBS.

Cell Isolation and Culture

Mouse embryonic fibroblasts were derived from B6 embryos (12.5–13.5 days postconception) (JAX C57BL/6J; The Jackson Laboratory). Cells were cultured in Dulbecco's modified Eagle's medium (DMEM) media, supplemented with fetal bovine serum (FBS) (10%), glutamax (2 mM), sodium pyruvate (1 mM), penicillin (100 units), streptomycin (100 μg/mL), non essential amino acids (0.10 mM) and monothioglycerol (MTG) (150 μM) at 37°C, 5% CO_2.

Fibroblasts were also derived from corneas of BALB/c mice by enzyme digestion and cultured in reduced serum medium (Opti-MEM; Invitrogen, Grand Island, NY), supplemented with FBS (4%), penicillin (2 units), and streptomycin (0.2 mg/mL). Briefly, corneas were hemisected and placed in sterile PBS containing 20 mM EDTA for 30 minutes at 37°C at which point the stroma was then separated from the epithelium. Stromal tissue was transferred into 1 mL of enzyme mixture (collagenase IV [10 mg/mL], dispase [50 U/mL], trypsin/EDTA [10 μL]) and incubated for 2 hours at 37°C with periodic vortexing. After centrifuging (10 minutes at 600*g*), cells were washed (2×) in PBS, then resuspended in media and plated at a density of 2.5×10^4 cells per cm^2.

In Vitro Stimulation Assay

Fibroblasts derived from B6 and BALB/c mice were stimulated with lipopolysaccharides (LPS) (25 μg/mL) (*P. aeruginosa* Serotype 10; Sigma, St. Louis, MO) + VIP (10^{-9} M) for 18 hours.[5] Supernatants were collected and assayed by real-time RT-PCR and ELISA for selected molecules associated with the ECM as described below.

Real-Time RT-PCR

Total RNA was isolated from individual corneas for in vivo analysis or collected from cell culture for in vitro analysis using an extraction reagent (RNA-Stat 60; Tel-Test, Friendsville, TX) according to the manufacturer's recommendations and was quantitated by spectrophotometric determination (260 nm). One microgram of total RNA was reverse transcribed as previously described.[5] All primer sets for PCR reactions were purchased either as a 96-well plate (RT^2 Profiler PCR Array; SABiosciences Corporation, Frederick, MD) or as individual primer sets (SABiosciences Corporation). Semiquantitative real-time RT-PCR was processed by a single color real-time RT-PCR detection system (MyiQ; Bio-Rad, Hercules, CA). PCR amplification conditions were set per the recommendations of SABiosciences Corporation. Relative transcript levels were calculated using the relative standard curve method that compares the amount of target normalized to an endogenous reference, β-actin. Briefly, the mean + SD values of replicate samples were calculated. Samples were then normalized to β-actin. Results are expressed as the relative amount of mRNA between experimental test samples and normal control samples (all normalized to β-actin). Before using this method, a validation experiment was performed comparing the standard curve of the reference and the target to demonstrate that efficiencies were approximately equal.

ELISA

Protein levels for select molecules associated with the ECM were tested using available ELISA kits (Integrin alpha 1, CD44, Laminin, Extracellular Matrix Protein 1, Versican, secreted phosphprotein 1; Antibodies-online Inc., Atlanta, GA). Corneas from VIP- and PBS-treated B6 mice and PBS-treated BALB/c mice were individually collected ($n = 5$/group/time point) under normal conditions and at 1 and 5 days PI for in vivo analysis. Samples were homogenized in 500 μL PBS with 0.1% Tween 20 and protease inhibitor cocktail tablets (containing protease inhibitors for serine, cysteine, and metalloproteases in bacterial, mammalian, yeast and plant cell extract) (cOmplete ULTRA Tablet; Roche, Mannheim, Germany). Supernatants were collected from in vitro stimulation assays (B6- and BALB/c-derived fibroblasts). All samples were centrifuged at 5000*g* (10 minutes), and an aliquot of each supernatant was assayed in triplicate for integrin, alpha 1 (ITG-α1), CD44, laminin 1 (LAMA-1), extracellular matrix protein 1 (ECM1), versican (VCAN) (VCAN is also known as chondroitin sulfate proteoglycan 2 [CSPG2]), and secreted phosphoprotein 1 (SPP1) according to the manufacturer's instruction. Assay sensitivity was <10 pg/mL (LAMA-1), <10 pg/mL (SPP1), <0.058 ng/mL (VCAN), <2.65 pg/mL (ITG-α1), 0.1 ng/mL (CD44), and 14.45 pg/mL (ECM1). Results are expressed either as average nanograms (or picograms)/cornea + SEM for in vivo and per mL for in vitro studies.

Immunofluorescent Staining

Expression of VIP receptor-1 (VIPR1) and VIP receptor-2 (VIPR2) by B6- and BALB/c-derived fibroblasts was evaluated by immunofluorescent staining using confocal laser scanning microscopy. Cells were cultured to subconfluency using glass culture slides (8-well CultureSlide; BD Biosciences, San Jose, CA). Sections were incubated with a nonspecific-fluorescence eliminator (Image-iT Signal Enhancer; Molecular Probes, Grand Island, NY) for 30 minutes at room temperature (RT). After blocking with 2.5% donkey serum (30 minutes, RT), slides were incubated with primary rabbit anti-VIPR1 (1/500) (VIP Receptor 1 Antibody; Novus Biologicals, Littleton, CO) or rabbit anti-VIPR2 (1/50) (VPAC2 Antibody; Novus Biologicals) for 1 hour, followed by AlexaFluor 594-conjugated donkey anti-rabbit IgG (1/200) (Alexa Fluor 594 Donkey Anti-Rabbit IgG [H+L]; Molecular Probes) for an additional hour. Slides were then incubated with a nucleic acid stain (1/5000) (SYTOX Green Nucleic Acid Stain; Invitrogen) for 2 minutes. Negative controls were similarly treated with species-specific IgG in lieu of primary antibodies. Sections were visualized, and digital images were captured using a confocal laser scanning microscope (TSC SP2; Leica Microsystems, Exton, PA).

Statistical Analysis

An unpaired Student's *t*-test was used to determine the significance of real-time RT-PCR and ELISA assays. Data were significant at $P < 0.05$. All experiments were repeated at least twice, and combined data from all replicates are shown unless otherwise indicated.

Results

VIP Treatment and In Vivo Expression of ECM Molecules

In an effort to uncover the effects of VIP treatment on corneal healing following bacterial keratitis, molecules associated with both degradation and restoration of the ECM and important for cell-matrix interactions were profiled by PCR array at 3 days PI in VIP- versus PBS-treated B6 mice. Tabulated results indicate

Table. Results from RT2 Proflier PCR Array

Symbol	Fold Up-/Down-Regulation VIP/PBS
CD44	8.08
CSPG2 (VCAN)	13.04
ECM1	−3.76
ITGA1	21.63
Integrin, alpha 2 (ITGA2)	8.17
Integrin, alpha L (ITGAL)	−6.87
Integrin, alpha M (ITGAM)	−4.18
Integrin, beta 1 (ITGB1)	−2.49
Integrin, beta 3 (ITGB3)	−4.11
LAMA1	4.91
Matrix metalloproteinase 2 (MMP)2	−7.92
Matrix metalloproteinase 9 (MMP)9	9.09
Matrix metalloproteinase 14 (MMP)14	8.31
Secreted protein acidic and rich in cysteine (SPARC)	−4.53
SPP1	−6.82

that VIP influences the matrix via differential expression of a number of different molecules (Table). While there are molecules that degrade the ECM, there are also factors that work in an opposite manner to promote proliferation and wound healing, thus restoring ECM structure and function. In this regard, select molecules from the Table were individually analyzed at the transcript level over time through 5 days PI in VIP- and PBS-treated B6 mice, and results are shown in Figure 1. Corneal mRNA expression levels for ITG-α1 (Fig. 1A) were increased significantly after VIP treatment at 1, 3, and 5 days PI. CD44, LAMA-1, ECM1, and VCAN mRNA levels were significantly up-regulated at 3 and 5 days PI (Figs. 1B–E). In contrast, SPP1 was significantly reduced over time following VIP treatment when compared to B6 wild-type (WT) controls (Fig. 1F).

Expression of all six molecules was further examined at the protein level by ELISA, and results are provided in Figures 2A–F. Changes in expression levels are not examined within groups, but between groups to illustrate the disparate expression profiles between "susceptible" B6 and "resistant" BALB/c mice and how VIP treatment alters the otherwise "normal" profile of the B6 response over time. Protein expression in the corneas of VIP- and PBS-treated B6 mice was assessed under normal conditions and at 1 and 5 days PI. Results were further compared to resistant BALB/c mice at the same time points to assess how well the disease response of VIP-treated B6 mice was ameliorated when compared to the naturally resistant response. Results at the protein level corroborated effects observed at the mRNA level between VIP-treated and WT B6 mice. Furthermore, ITG-α1 (Fig. 1A), CD44 (Fig. 1B), LAMA-1 (Fig. 1C), ECM1 (Fig. 1D), VCAN (Fig. 1E), and SPP1 (Fig. 1F) expression after VIP treatment displayed trends that strongly paralleled those levels observed in resistant BALB/c mice following infection.

Effects of VIP Treatment on B6- versus BALB/c-derived Fibroblasts In Vitro

Given the dichotomy of disease response between B6 (cornea perforates) and BALB/c (cornea heals) mice and that VIP treatment resulted in enhanced expression of ECM molecules associated with healing in B6 mice after infection with *P. aeruginosa*, we next examined whether fibroblasts from the two mouse strains respond differently to the presence of VIP. Therefore, both B6- and BALB/c-derived fibroblasts were used to directly determine the effects of VIP treatment on expression of ECM molecules in vitro. These cells were stimulated with LPS (25 μg/mL) and/or VIP 10^{-9} M, then tested for ITG-α1, CD44, LAMA-1, ECM1, VCAN, and SPP1 expression at the transcript (Fig. 3) and protein (Fig. 4) levels at 18 hours poststimulation. Results indicated that BALB/c-derived fibroblasts expressed more mRNA for ITG-α1, CD44, LAMA-1, ECM1, and VCAN (Figs. 3A–E) when compared to B6-derived cells for all treatment groups (LPS only, VIP only, and LPS + VIP). Messenger RNA for SPP1, however, was significantly higher in B6-derived fibroblasts versus BALB/c (Fig. 3F).

When examined at the protein level, ITG-α1, CD44, LAMA-1, and VCAN (Figs. 4A–C, 4E, respectively) were significantly higher under normal conditions in BALB/c-derived fibroblasts versus B6; ECM1 (Fig. 4D) showed no difference. After LPS stimulation, ITG-α1, CD44, and LAMA-1 remained significantly elevated in BALB/c versus B6, while there were no differences for ECM1 and VCAN. In contrast, SPP1 remained significantly higher in B6-derived fibroblasts compared to BALB/c for all groups (Fig. 4F). Most notable, though, was that all molecules were significantly elevated in fibroblasts from both strains when VIP was present (either VIP alone or LPS + VIP) when compared to LPS alone (e.g., B6 LPS + VIP compared to B6 LPS only).

VIPR1/VIPR2 Expression in B6- versus BALB/c-derived Fibroblasts

Studies have demonstrated that, in regard to MΦ, many of the VIP-induced effects are primarily carried out through VIPR1.[5,6] In this regard, we have previously shown that there is both differential expression of VIPR1 on this cell type as well as a differential response to VIP between B6 and BALB/c mice, thus contributing to the differences observed in disease pathogenesis. Our current in vivo and in vitro data also suggest a differential response to VIP between B6 and BALB/c mice in regard to expression of ECM molecules. Therefore, both VIPR1 and VIPR2 were further examined at the mRNA level in B6- and BALB/c-derived fibroblasts (Figs. 5A, 5B). Unstimulated fibroblasts from both strains showed constitutive expression of VIPR1 and VIPR2; however VIPR1 levels were significantly higher in B6 mice, while VIPR2 was significantly elevated in BALB/c. After LPS stimulation, both VIPR1/2 remained up-regulated in BALB/c and B6 cell lines, yet again fibroblasts from B6 mice showed more VIPR1 mRNA, while BALB/c expressed more VIPR2. This trend (more VIPR1 in B6; more VIPR2 in BALB/c) was maintained after VIP treatment alone and after LPS + VIP treatment.

Next, VIPR1/2 expression in B6- and BALB/c-derived fibroblasts was examined in vitro using fluorescent confocal laser scanning microscopy (Fig. 6). Negative controls (primary antibodies omitted) indicated no detectable $VIPR1^+$ or $VIPR2^+$ immunostaining (red) (Figs. 6A, 6F, 6K, 6P). Under normal conditions (no treatment), VIPR1 was predominantly detected near the nucleus of B6-derived fibroblasts (Fig. 6L). In BALB/c fibroblasts, VIPR1 expression was detected throughout the entire cell body (Fig. 6B), suggesting possible receptor association with both the cell membrane and throughout the cytoplasm. However, VIPR1 staining was observed both throughout the cell body and around the nucleus in BALB/c and B6 cells with VIP treatment only (Fig. 6C, BALB/c; Fig. 6M, B6), after LPS stimulation (Fig. 6D, BALB/c; Fig. 6N, B6), and following both LPS + VIP (Fig. 6E, BALB/c; Fig. 6O, B6). Furthermore, VIPR1 staining appeared most prominent throughout the cell body of B6-derived fibroblasts following VIP exposure, as shown in Figure 6M (VIP treatment only) and Figure 6O (VIP + LPS).

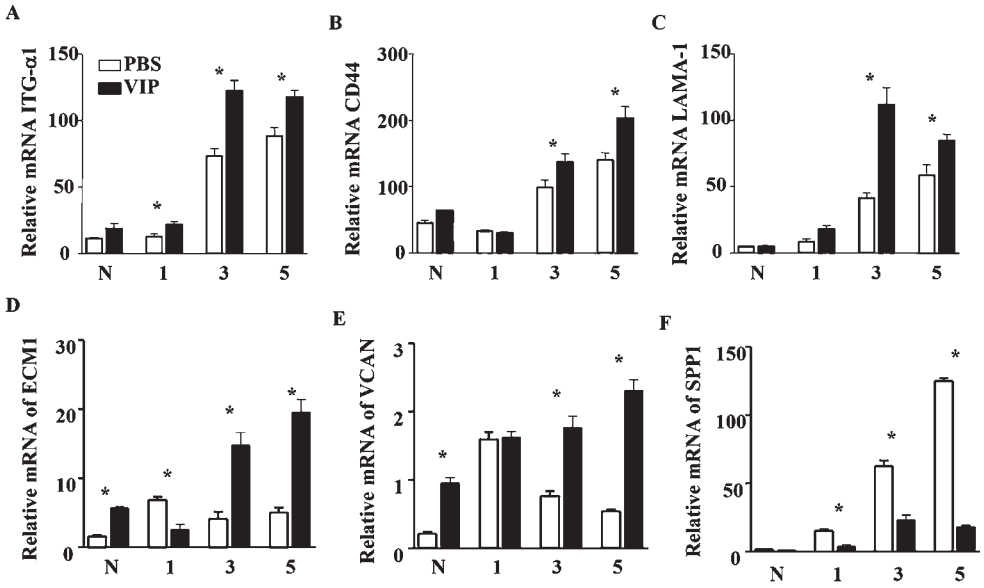

Figure 1. ECM molecule transcript levels as detected by real-time RT-PCR in VIP- versus PBS-treated B6 corneas after ocular infection. ITG-α1 (**A**) levels were significantly elevated with VIP treatment at 1, 3, and 5 days PI, while CD44 (**B**), LAMA-1 (**C**), ECM-1 (**E**), and VCAN (**F**) levels were significantly enhanced 3 and 5 days PI when compared to PBS controls. VIP treatment significantly reduced SPP-1 (**F**) at 1, 3, and 5 days PI. * ITG-α1: $P = 0.04$ (day 1), < 0.001 (day 3), $= 0.003$ (day 5); CD44: $P = 0.040$ (day 3) and 0.004 (day 5); LAMA-1: $P < 0.001$ (day 3) and $= 0.022$ (day 5); ECM1: $P < 0.001$ (N, day 1, day 3, day 5); VCAN: $P < 0.001$ (N, day 3, day 5); SPP1: $P < 0.001$ (day 1, day 3, day 5).

Contrary to VIPR1 immunostaining, VIPR2 appeared to be restricted to the nucleus of both BALB/c- and B6-derived fibroblasts under normal conditions (Figs. 6G, 6Q, respectively). After exposure to VIP (VIP only and LPS + VIP treatment groups), both cell body and nuclear staining were observed in both cell lines (BALB/c: Figs 6H, 6J; B6: Figs. 6R, 6T). Most interesting, however, was that VIPR2 staining appeared limited to the nucleus of both BALB/c- and B6-derived fibroblasts after

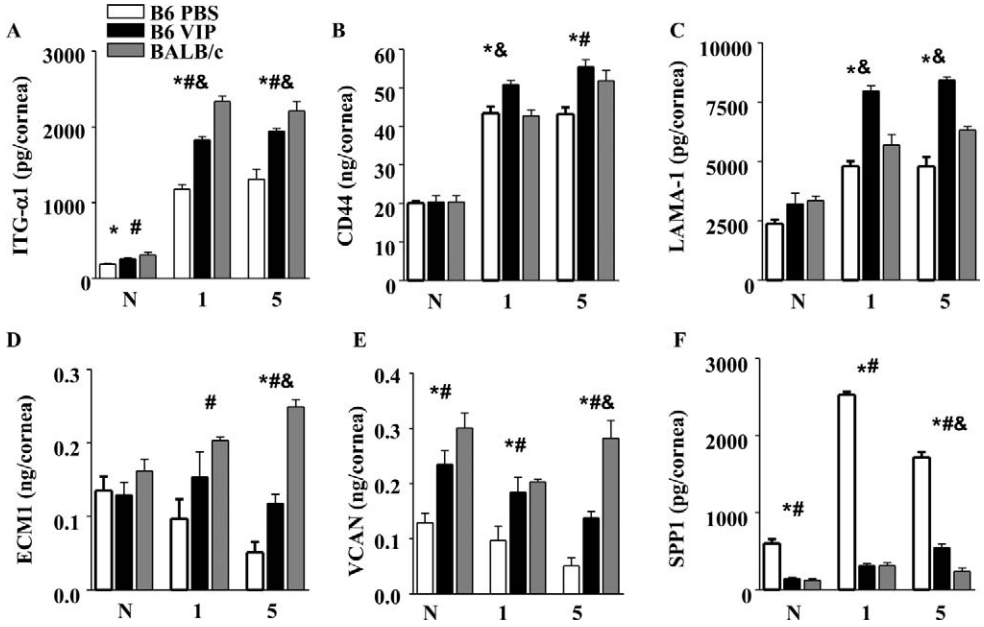

Figure 2. ECM molecule protein levels as detected by ELISA in VIP-treated B6, PBS-treated B6, and PBS-treated BALB/c corneas under normal conditions and at 1 and 5 days after infection. ITG-α1 (**A**), CD44 (**B**), LAMA-1 (**C**), ECM1 (**D**), and VCAN (**E**) protein levels were significantly elevated in VIP-treated corneas over time when compared to PBS-treated B6 mice. In addition, VIP treatment showed similar trends to protein levels normally detected in PBS-treated BALB/c corneas after infection. SPP1 (**F**), in contrast, was significantly decreased (similar to PBS-treated BALB/c) after VIP treatment when compared to PBS B6 controls. * ITG-α1: $P = 0.01$ (N), < 0.001 (day 1), $= 0.004$ (day 5); CD44: $P = 0.007$ (day 1), $= 0.01$ (day 5); LAMA-1: $P < 0.001$ (day 1, day 5); ECM1: $P = 0.007$ (day 5); VCAN: $P = 0.01$ (N), $= 0.04$ (day 1), $= 0.002$ (day 5); SPP1: $P = 0.02$ (N), < 0.001 (day 1, day 5) for VIP versus PBS B6. # ITG-α1: $P = 0.02$ (N), < 0.001 (day 1), $= 0.002$ (day 5); CD44: $P = 0.028$ (day 5); ECM1: $P = 0.02$ (day 1), < 0.001 (day 5); VCAN: $P = 0.002$ (N), $= 0.023$ (day 1), < 0.001 (day 5); SPP1: $P = 0.019$ (N), < 0.001 (day 1, day 5) for PBS B6 versus PBS BALB/c. & ITG-α1: $P = 0.002$ (day 1), $= 0.008$ (day 5); CD44: $P = 0.004$ (day 1); LAMA-1: $P = 0.004$ (day 1), < 0.001 (day 5); ECM1: $P < 0.001$ (day 5); VCAN: $P = 0.002$ (day 5); SPP1: $P = 0.008$ (day 5) for VIP versus PBS BALB/c.

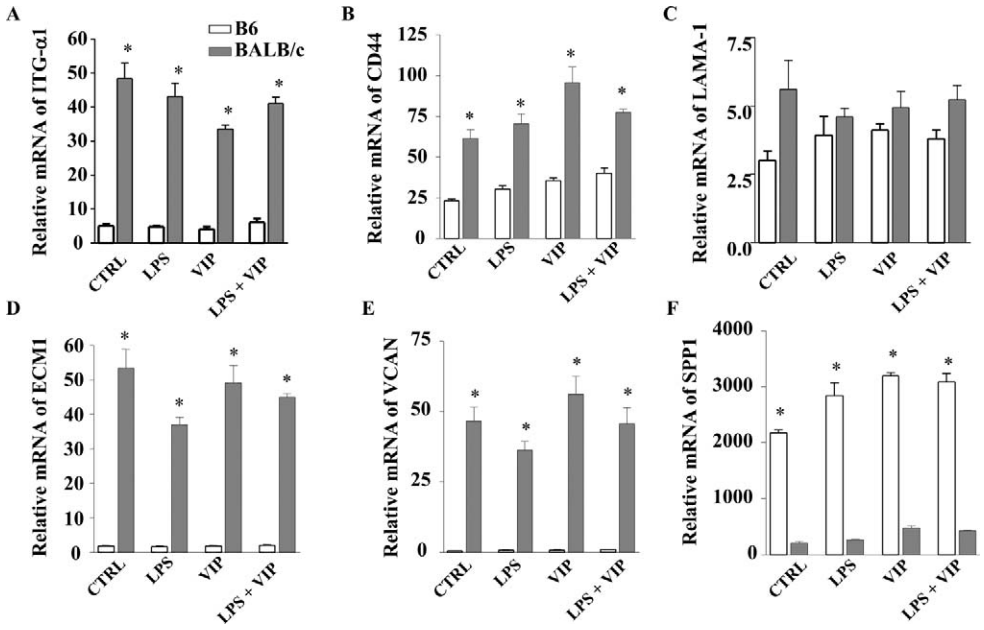

Figure 3. In vitro effects of VIP treatment on ECM mRNA expression levels from B6- and BALB/c-derived fibroblasts. Fibroblasts were stimulated with LPS (25 μg/mL) + VIP treatment (10^{-9} M) for 18 hours. The relative mRNA levels of ITG-α1 (**A**), CD44 (**B**), LAMA-1 (**C**), ECM1 (**D**), VCAN (**E**), and SPP1 (**F**) were determined by real-time RT-PCR. *$P < 0.001$.

LPS stimulation only (no VIP treatment) as shown in Figures 6I, 6S, respectively.

Discussion

Our laboratory has demonstrated VIP capable of converting disease outcome in a murine model of *P. aeruginosa*-induced ocular infection. Effects include a robust anti-inflammatory influence over cytokine/chemokine production, predominately through transforming growth factor (TGF)-β, decreased expression of adhesion molecules leading to reduced inflammatory cell infiltration and persistence in the cornea, and enhanced expression of growth factors known to facilitate wound healing.[5,7,10] In light of the aforementioned evidence supporting VIP as a multifaceted neuropeptide, it led to the current investigation into how VIP may further modulate disease pathogenesis through ECM regulation and restoration, ultimately leading to corneal homeostasis.

As such, it was revealed that VIP treatment of B6 mice enhanced the expression of a number of molecules (when compared to WT B6 controls) that typically contribute to the restoration of the matrix, specifically ITG-α1. Integrins are a family of cell-surface glycoproteins that form heterodimers

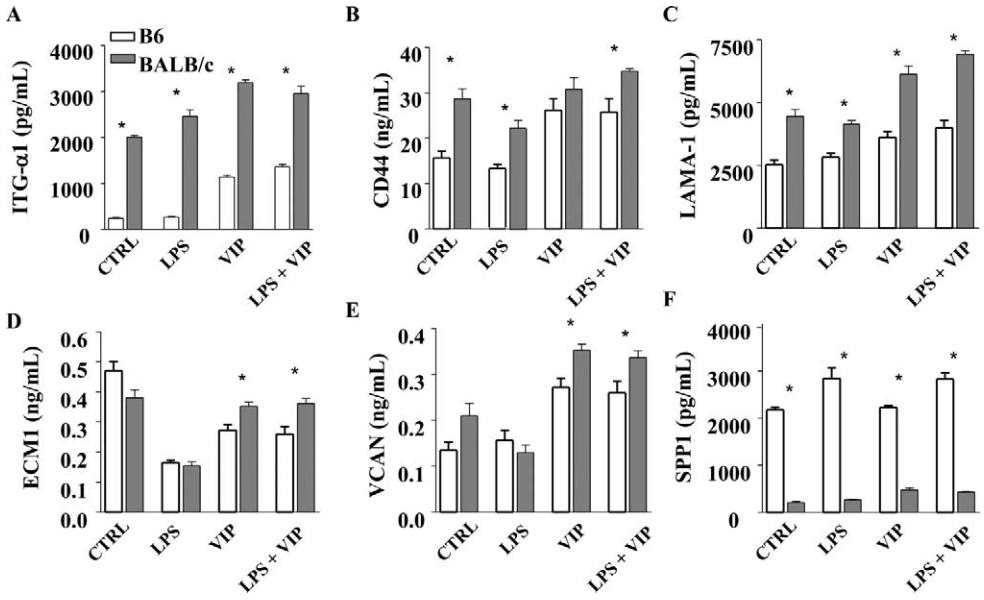

Figure 4. In vitro effects of VIP treatment on ECM protein levels from B6- and BALB/c-derived fibroblasts. Fibroblasts were stimulated with LPS (25 μg/mL) + VIP treatment (10^{-9} M) for 18 hours. Protein levels of ITG-α1 (**A**), CD44 (**B**), LAMA-1 (**C**), ECM1 (**D**), VCAN (**E**), and SPP1 (**F**) were determined by ELISA. * ITG-α1: $P < 0.001$ (all groups); CD44: $P = 0.002, = 0.001, = 0.04, = 0.03$; LAMA-1: $P < 0.001$ (all groups); ECM1: $P = 0.041, = 0.028$; VCAN: $P = 0.016, = 0.037$; SPP1: $P < 0.001$ (all groups).

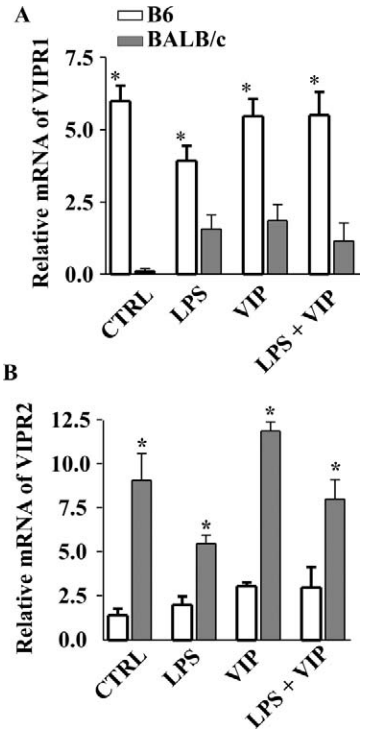

Figure 5. Expression of VIPR1 and VIPR2 mRNA in B6- and BALB/c-derived fibroblasts. Cells were stimulated with LPS (25 μg/mL) + VIP treatment (10^{-9} M) for 18 hours, and transcript levels were determined by real-time RT-PCR. (**A**) Higher levels of VIPR1 mRNA were detected in B6-derived fibroblasts when compared to BALB/c regardless of treatment group. (**B**) VIPR2 mRNA was enhanced in BALB/c-derived fibroblasts when compared to B6 in all treatment groups. $^*P < 0.001$.

composed of individual α and β chains.[11] These molecules function as receptors for ECM proteins such as fibronectin, vitronectin, osteopontin, various laminins, and collagens, mediating cell-cell and cell-ECM interactions, and they are in constant communication with the ECM environment.[11–13] Integrins α1β1 and α2β1 often have been cited as the canonical integrin collagen receptors.[11,14] Studies analyzing the dermal wound response of mice expressing a null mutation of the α1 subunit revealed that this molecule participates in the normal feedback regulation of collagen synthesis and in collagen-mediated cell proliferation.[15,16] After VIP treatment, corneal transcript levels of both α1 and α2 integrins were significantly elevated over WT B6 as detected by PCR array (Table). Alpha-1 integrin was further shown to be increased at the protein level both in vivo and in vitro, thus supporting the role for these molecules in wound healing and as promoters of matrix stability. In contrast to α1 and α2 (members of the β1 integrin family), αL is a β2 integrin, which functions primarily in immune cells.[11] Alpha-L forms the αLβ2 heterodimer and under increased LPS concentrations, serves as an additional receptor to CD14. As expected, this molecule was reduced in VIP- versus PBS-treated B6 animals (Table).

CD44 is a type I transmembrane glycoprotein that regulates conformational changes of integrin heterodimers and their ability to microcluster and anchor to the actin cytoskeleton.[17,18] Recent studies using a mouse model of spontaneously metastasizing breast cancer have provided evidence that CD44 is protective against metastasis.[19] The authors demonstrated that the loss of CD44, in fact, promoted metastasis to the lung and that inhibition of the CD44-hyaluronan association increased invasion of tumor cells.[19] These results suggest that epithelial-stromal interactions via CD44 are protective against cellular infiltration/invasion of the ECM. VIP treatment resulted in a significant up-regulation of CD44 mRNA and protein in the whole cornea when compared to PBS-treated B6 controls. This effect was also demonstrated in fibroblasts in vitro. These data strengthen the idea that CD44 functions to preserve and restore functional integrity of the corneal stroma, while regulating cellular infiltration.

Laminins are a family of glycoproteins, composed of three chains (α, β, and γ) that are secreted and incorporated into the cell-associated ECM. These molecules are an essential component of the structural scaffolding of basement membranes. Of the approximately 15 laminin trimers, laminin-1 expression appears to be largely associated with epithelial basement membranes. Laminin-1 forms independent networks that join together with collagen networks via perlecan and other associated proteins.[20] In addition, laminin-1 binds to cell membranes via integrin receptors and other molecules of the plasma membrane. Through these interactions, laminins greatly contribute to cell attachment/differentiation, cell shape/movement, maintenance of tissue phenotype, and promotion of tissue survival.[21] Treatment with VIP revealed an up-regulation in corneal laminin-1 mRNA and protein expression when compared to PBS-treated B6 controls when examined both in vivo (whole cornea) and in vitro (fibroblasts). These data suggest that VIP promotes epithelial cell development and basement membrane integrity through the expression of laminin-1 and potentially other laminins, as well.

In addition, both ECM1 and VCAN (CSPG2) expression was increased in the whole cornea (in vivo) and in fibroblasts (in vitro) when stimulated with VIP. ECM1 is a soluble protein known to interact with a variety of extracellular and structural proteins, which contributes to tissue integrity and homeostasis[22] while VCAN, a large chondroitin sulfate proteoglycan, is a major component of the ECM. This molecule is involved in cell proliferation, cell migration, tissue morphogenesis, and tissue maintenance, and it may play a role in intercellular signaling within the matrix.[23]

Parallel to the increased expression of molecules associated with the restoration and maintenance of the ECM, VIP treatment resulted in decreased expression of SPP1, demonstrated both in vivo (compared to PBS-treated B6 controls) and in vitro. SPP1 is associated with enhancing the T helper cell 1 (Th1) pathway and has been shown to enhance IFN-γ and IL-12 production, while reducing IL-10. It is expressed on a multitude of immune cells (MΦ, neutrophils, dendritic cells, T and B cells) and is a chemoattractant for both neutrophils and MΦ.[24]

VIP is known to function predominately through two receptors: VIPR1 (VPAC1) and VIPR2 (VPAC2). In this regard, we have previously demonstrated that the anti-inflammatory effects of VIP are carried out primarily through VIPR1—receptor expression is more prominent on BALB/c versus B6 MΦ and dose dependent—BALB/c endogenously express more VIP than B6, contributing to the predisposition of BALB/c mice toward resistance.[5] To this end, in the current study we also examined whether fibroblasts showed a higher propensity for VIPR1 versus VIPR2 expression in general, and if so, whether the receptor was differentially expressed between B6 and BALB/c mice. VIPR1 mRNA was higher in B6- versus BALB/c-derived fibroblasts under normal conditions. However, immunostaining revealed that VIPR1 was generally expressed throughout the cell body of BALB/c fibroblasts, while in B6 cells VIPR1 appeared focused around the nucleus. In fact, positive staining was consistently detected throughout the cell body for all treatment groups in BALB/c-derived fibroblasts. After LPS stimulation of B6-derived fibroblasts, VIPR1 was detected in the cell body, yet still appeared focused at the nucleus. VIP treatment, however, resulted in more VIPR1

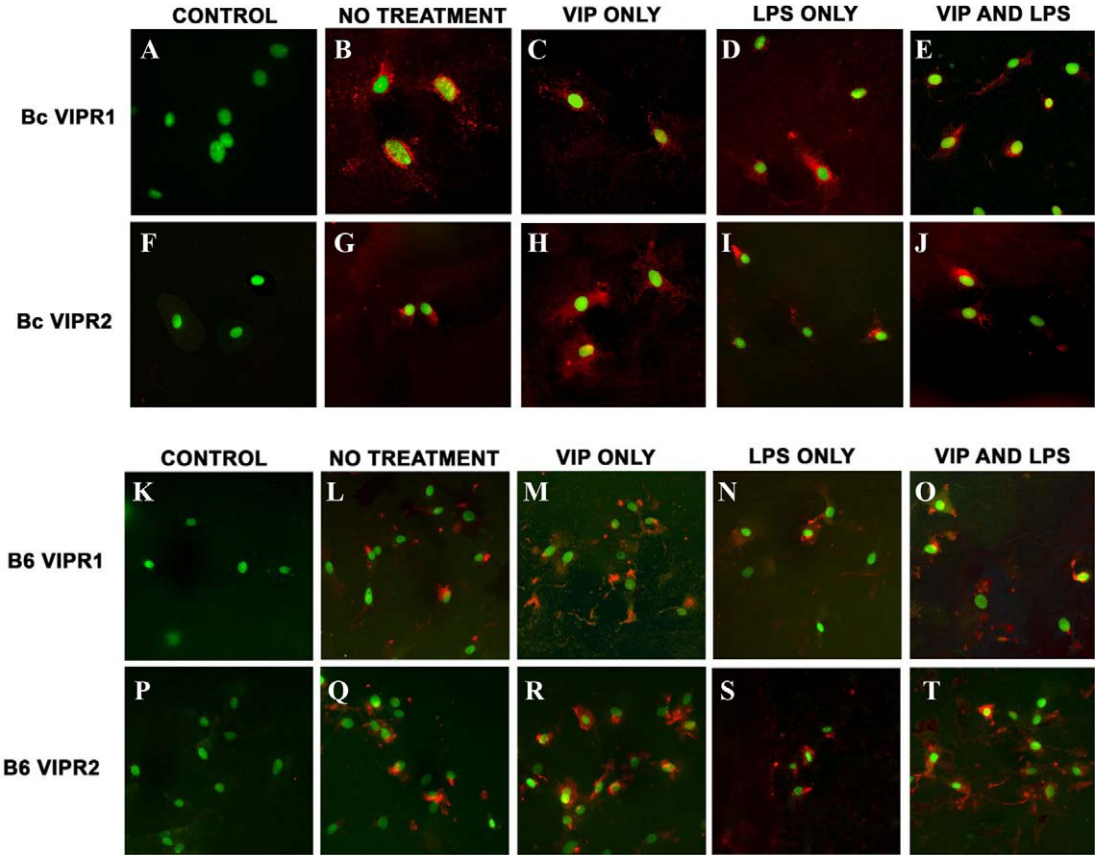

Figure 6. Immunostaining for VIPR1 and VIPR2 in BALB/c- and B6-derived fibroblasts after in vitro stimulation. Cells were stimulated with LPS (25 μg/mL) + VIP treatment (10^{-9} M) for 18 hours, and receptor expression was determined by confocal laser scanning microscopy. Positive staining (red) for VIPR1$^+$ and VIPR2$^+$ BALB/c-derived fibroblasts are provided in (**B–E**) and (**G–J**), respectively, and for B6-derived fibroblasts in (**L–O**) for VIPR1$^+$ and (**Q–T**) for VIPR2$^+$. Primary antibody was replaced with species-specific IgG in control sections, which were positive for SYTOX Green nuclear stain only (**A**, **F**, **K**, **P**).

staining observed in the cell body (versus nucleus) of B6-derived fibroblasts—suggesting that increased VIP (which is endogenously higher in BALB/c, lower in B6) may induce the translocation of VIPR1. Therefore, we speculate that without "adequate" levels of VIP, VIPR1 remains localized to the nucleus and ultimately leads to a more mis-regulated inflammatory response since this receptor (and subsequent pathway) is not as readily available/active, thus giving way to the susceptible phenotype observed in the B6 mouse.

Most notably, immunostaining further suggests that VIPR2 may carry out the healing effects of VIP. Contrary to VIPR1, VIPR2 staining appeared largely confined to the nucleus after LPS stimulation in both B6- and BALB/c-derived fibroblasts. However, after VIP exposure in both strains, VIPR2 was detected throughout the cell body. We hypothesize that in the presence of LPS, the cell is focused on inflammation and bacterial killing (which is carried out by VIPR1) as opposed to immune homeostasis and tissue restoration. We further surmise that once VIP is present at "high enough" levels, the cell shifts from an active inflammatory response to healing. As a result, VIPR2 expression extends throughout the cell body in an attempt to execute the VIP-induced effects to restore tissue integrity and corneal homeostasis. However, these interpretations remain to be substantiated by future receptor antagonist and/or receptor knock-out studies.

Understanding disease pathogenesis regarding bacterial keratitis involves elucidating a number of different components. This includes mechanisms of inflammation, as well as corneal healing and restoration. Through delineation of these pathways, we can explicitly target certain aspects of disease pathogenesis, for example, by using specific receptor agonists/antagonists or exogenously enhancing the production of those molecules known to constitute a major role during the healing process. The findings garnered through the current study support the main hypothesis that VIP is an immunomodulatory neuropeptide that promotes not only anti-inflammatory events but ultimately functions to restore immune homeostasis. Moreover, this conclusion is relevant to therapeutic intervention and the design of new pharmacological approaches not limited to ocular infections, but to diseases including sepsis, skin disorders, asthma, rheumatoid arthritis, and other inflammatory disorders.

References

1. Rattanatam T, Heng WJ, Rapuano CJ, Laibson PR, Cohen EJ. Trends in contact lens-related corneal ulcers. *Cornea*. 2001; 20:290–294.
2. Murillo-Lopez FH. Bacterial keratitis clinical presentation. *The Medscape from WebMD Journal of Medicine* [online]. 2011. Available at: http://emedicine.medscape.com/article/1194028. Accessed September 25. 2011.
3. Stapleton F, Keay L, Edwards K, et al. The incidence of contact lens-related microbial keratitis in Australia. *Ophthalmology*. 2008;115:1655–1662.
4. Hall BJ, Jones L. Contact lens cases: the missing link in contact lens safety? *Eye Contact Lens*. 2010;36:101–105.

5. Szliter EA, Lighvani S, Barrett RP, Hazlett LD. Vasoactive intestinal peptide balances pro- and anti-inflammatory cytokines in the Pseudomonas aeruginosa-infected cornea and protects against corneal perforation. *J Immunol*. 2001;178:1105–1114.
6. Leceta J, Gomariz RP, Martinez C, Abad C, Ganea D, Delgado M. Receptors and transcriptional factors involved in the anti-inflammatory activity of VIP and PACAP. *Ann N Y Acad Sci*. 2000;921:92–102.
7. Berger EA, McClellan SA, Barrett RP, Hazlett LD. VIP promotes resistance in the Pseudomonas aeruginosa infected cornea by modulating adhesion molecule expression. *Invest Ophthalmol Vis Sci*. 2010;51:5776–5782.
8. Dong Z, Ghabrial M, Katar M, Fridman R, Berk RS. Membrane-type matrix metalloproteinases in mice intracorneally infected with Pseudomonas aeruginosa. *Invest Ophthalmol Vis Sci*. 2000;41:4189–4194.
9. Rudner XL, Kernacki KA, Barrett RP, Hazlett LD. Prolonged elevation of IL-1 in *Pseudomonas aeruginosa* ocular infection regulates macrophage-inflammatory protein-2 production, polymorphonuclear neutrophils persistence, and corneal perforation. *J Immunol*. 2000;164:6576–6582.
10. Jiang X, McClellan SA, Barrett RP, Berger EA, Zhang Y, Hazlett LD. VIP regulates growth factors to promote healing in the infected cornea. *Invest Ophthalmol Vis Sci*. 2011;52:6154–6161.
11. Stepp, MA, Zhu L, Cranfill R. Changes in beta 4 integrin expression and localization in vivo in response to corneal epithelial injury. *Invest Ophthalmol Vis Sci*. 1996;37:1593–1601.
12. Aplin AE, Howe A, Alahari SK, Juliano RL. Signal transduction and signal modulation by cell adhesion receptors: the role of integrins, cadherins, immunoglobulin-cell adhesion molecules, and selectins. *Pharmacol Rev*. 1998;50:197–263.
13. Hynes RO. Integrins: versatility, modulation, and signaling in cell adhesion. *Cell*. 1992;69:11–25.
14. Wayner EA, Carter WG. Identification of multiple cell adhesion receptors for collagen and fibronectin in human fibrosarcoma cells possessing unique alpha and common beta subunits. *J Cell Biol*. 1987;105:1873–1884.
15. Gardner CR, Laskin JD, Laskin DL. Distinct biochemical responses of hepatic macrophages and endothelial cells to platelet-activating factor during endotoxemia. *J Leukoc Biol*. 1995;57:269–274.
16. Pozzi A, Wary KK, Giancotti FG, Gardner HA. Integrin alpha1beta1 mediates a unique collagen-dependent proliferation pathway in vivo. *J Cell Biol*. 1998;142:587–594.
17. Carman CV, Springer TA. Integrin avidity regulation: are changes in affinity and conformation underemphasized? *Curr Opin Cell Biol*. 2003;15:547–556.
18. Shamri R, Grabovsky V, Gauguet JM, et al. Lymphocyte arrest requires instantaneous induction of an extended LFA-1 conformation mediated by endothelium-bound chemokines. *Nat Immunol*. 2005;6:497–506.
19. Lopez JI, Camenisch TD, Stevens MV, Sands BJ, McDonald J, Schroeder JA. CD44 attenuates metastatic invasion during breast cancer progression. *Cancer Res*. 2005;65:6755–6763.
20. Timpl R, Brown JC. Supramolecular assembly of basement membranes. *Bioessays*. 1996;18:123–132.
21. Ekblom P, Lonai P, Talts JF. Expression and biological role of laminin-1. *Matrix Biol*. 2003;22:35–47.
22. Sercu S, Zhang L, Merregaert J. The extracellular matrix protein 1: its molecular interaction and implication in tumor progression. *Cancer Invest*. 2008;26:375–384.
23. Chiodoni C, Colombo MP, Sangaletti S. Matricellular proteins: from homeostasis to inflammation, cancer, and metastasis. *Cancer Metastasis Rev*. 2010;29:295–307.
24. Glas J, Seiderer J, Bayrle C, et al. The role of osteopontin (OPN/SPP1) haplotypes in the susceptibility to Crohn's disease. [published online ahead of print December 29, 2011] *PLoS One*. 2011;6:e29309.